Open access • Journal Article • DOI:10.1093/JAC/DKW003

Whole-genome typing and characterization of blaVIM19-harbouring ST383 Klebsiella pneumoniae by PFGE, whole-genome mapping and WGS

Julia Sabirova, Basil Britto Xavier, Jasmine Coppens, Olympia Zarkotou ...+6 more authors

Institutions: University of Antwerp

Published on: 01 Jun 2016 - Journal of Antimicrobial Chemotherapy (Oxford University Press)

Whole-genome typing and characterization of bla_{VIM19}-harbouring ST383 Klebsiella pneumoniae by PFGE, whole-genome mapping and WGS

Whole genome typing and characterisation of bla$_{VIM19}$-harbouring ST383 *Klebsiella pneumoniae* by PFGE, whole genome mapping and sequencing

Julia S. Sabirova[a*], Basil Britto Xavier[a*], Jasmine Coppens[a], Olympia Zarkotou[b], Christine Lammens[a], Lore Janssens[a], Ronald Burggrave[c], Trevor Wagner[c], Herman Goossens[a], Surbhi Malhotra-Kumar[a#]

[a]Department of Medical Microbiology, Vaccine & Infectious Disease Institute, Universiteit Antwerpen, Antwerp, Belgium[a]; Department of Microbiology, Tzaneio General Hospital, Piraeus, Greece[b]; OpGen, Inc., Gaithersburg, Maryland, USA[c].

Running Title: bla$_{VIM19}$-harbouring ST383 *K. pneumoniae*

Key words: Whole genome sequencing, class 1 integron, integrase, *ICEPm1*, ST383, optical mapping, whole genome maps, PFGE

Text word count: 3749

Synopsis word count: 248

*Equal contribution authors

[#]Corresponding author mailing address: Department of Medical Microbiology, Campus Drie Eiken, University of Antwerp, S6, Universiteitsplein 1, B-2610 Wilrijk, Belgium. Phone: 32-3-265-27-52. Fax: 32-3-265-26-63. E-mail: surbhi.malhotra@uantwerpen.be

Synopsis

Objectives: We utilized whole-genome mapping (WGM) and WGS to characterize 12 clinical carbapenem-resistant *Klebsiella pneumoniae* (TGH1-TGH12).

Methods: All strains were screened for carbapenemase genes by PCR, and typed by MLST, PFGE (*XbaI*), and WGM (*AflII)* (Opgen, USA). WGS (Illumina) was performed on TGH8 and TGH10. Reads were *denovo* assembled and annotated (SPAdes, RAST). Contigs were aligned directly, and after *in silico AflII* restriction, with corresponding WGMs (MapSolver, OpGen; BioNumerics, Applied Maths).

Results: All 12 strains were ST383. Eleven of the 12 strains were carbapenem-resistant and 7 harboured $bla_{\text{KPC-2,}}$ and 11, $bla_{\text{VIM-19 .}}$ Varying the parameters for assigning WGM clusters showed that these were comparable to ST types, and to the 8 PFGE (sub)types (≥ 3-band difference). A 95% similarity coefficient assigned all 12 WGMs to a single cluster while a 99% similarity coefficient (or ≥ 10 unmatched-fragment difference) assigned the 12 WGMs to 8 (sub)clusters. Based on a ≥ 3-band difference between PFGE profiles, the Simpson's diversity index (SDI) of WGM (0.94, Jackknife pseudo-values CI: 0.883-0.996) and PFGE (0.93, CI: 0.828-1.000) were similar (p=0.649). However, discriminatory power of WGM was significantly higher (SDI: 0.94, CI: 0.883-0.996) than PFGE profiles typed on a ≥7-band difference (SDI: 0.53, CI: 0.212-0.849) (p=0.007).

Conclusions: This study demonstrates the application of whole-genome mapping to understanding the epidemiology of hospital-associated *K. pneumoniae*. Utilizing a combination of WGM and WGS, we also present here the first longitudinal genomic characterization of the highly dynamic carbapenem-resistant ST383 *K. pneumoniae* clone that is rapidly gaining importance in Europe.

INTRODUCTION

The spread of multidrug-resistant *K. pneumoniae* strains in hospitals constitutes a pressing global health problem. The increasing prevalence of plasmid-encoded carbapenem-hydrolysing enzymes in *K. pneumoniae* is of particular concern due to their ability to hydrolyse almost all β-lactam antibiotics, as well as their genetic association with transferable multidrug resistance.[1-3] Infections due to carbapenem-resistant *K. pneumoniae* are not only difficult to treat due to limited therapeutic options, but such clones could potentially cause hospital epidemics if not promptly detected and contained.[4]

Molecular typing techniques are effective surveillance tools to monitor the dynamics of multidrug-resistant clones circulating in hospitals during non-outbreak situations and to detect early signs of an outbreak. Currently used techniques are based on amplification of marker genes followed by sequencing (MLST), or targeting entire genomes by PFGE or by whole genome mapping (WGM), with the restriction fragments analysed on a gel or in a microfluidic device, respectively. Of the three techniques, MLST is most commonly utilized for bacteria strain typing. While it is highly reproducible and relatively inexpensive, the resolution achieved by clustering strains based on sequenced segments of seven or more housekeeping genes is not high enough to study inter- and intra-clonal genetic diversity. Compared to PFGE, WGM has the advantage of being less labour intensive and, importantly, allowing inter-lab reproducibility and comparison of results that has been a major shortcoming of PFGE typing. WGM is also far less technologically challenging than whole genome sequencing (WGS) and does not require bioinformatics expertise. Furthermore, results can be generated on the same day with WGM that offers a distinct advantage for microbiology laboratories undertaking outbreak investigations. Notwithstanding instrument costs, the cost of running a single strain for PFGE < WGM ≤ WGS. Also with WGM, the genetic content of the detected variable genome regions can be extracted and identified by utilizing the vast number of publicly available whole genome sequences. These can be utilized to develop *in*

silico restriction maps using the same enzymes as used for experimentally-generated WGMs, allowing comparison of restriction patterns and eventual identification of the genetic content of the variable regions in the strains of interest.[5]

In this study, we demonstrate the utility of WGM in conjunction with WGS for typing, characterizing, and dissecting the genomic features of carbapenem-resistant *K. pneumoniae* isolated at the Tzaneio General (TG) hospital, Piraeus, Greece. Carbapenem-resistant *K. pneumoniae* producing VIM-type metallo-β-lactamases have been endemic in Greek hospitals since the early 2000s.[6] Many strains with VIM-1–producing *K. pneumoniae* have also been described.[7] From 2007, KPC-type carbapenemases became prevalent and even caused outbreaks,[8, 9] followed by emergence of strains coproducing KPC and VIM.[10] We studied VIM- and KPC-+VIM-producing *K. pneumoniae* isolated from colonized or infected patients during 2010-2013 at the TG hospital.

MATERIALS AND METHODS

Strain collection

Twelve *K. pneumoniae* (TGH1-TGH12), harbouring bla_{VIM} and/or bla_{KPC}, and isolated from patients admitted to the intensive care unit (n=8) or surgical ward (n=4) at the TG hospital during 2010-2013 were studied. Clinical data and strain characteristics are outlined in Table 1.

Antimicrobial resistance profiling

All 12 strains were screened for resistance to 17 antibiotics, including β-lactams with and without β-lactamase inhibitors, by disk diffusion (Table 1). MICs of carbapenems (ertapenem, imipenem and meropenem) were determined by Etest (bioMérieux Inc., Durham, NC), and results interpreted according to CLSI cut-offs. [11] Strains were screened for presence of extended-spectrum β-lactamase (ESBL) and carbapenemase genes by PCR and Sanger sequencing as described previously.[12-14]

MLST and PFGE

MLST was performed as described previously for seven marker genes (*gapA*, *infB*, *mdh*, *pgi*, *phoE*, *rpoB*, *tonB*),[15] and sequence types were assigned using the Institute Pasteur database (www.pasteur.fr/mlst). PFGE was performed as follows. Briefly, cells from an overnight blood agar culture were washed, adjusted to a density of 1.0 OD at 600nm in EC lysis buffer (100 mM EDTA, 5M NaCl, 0.5% Brij-58, 0.2% deoxycholate, 10% N-laurylsarcosine, 6 mM Tris–HCl pH 7.6), and after centrifugation, resuspended into 200µL EC lysis buffer with 10 µL proteinase K (20mg/mL). Cell suspension was mixed with equal volume of 1.0% (w/v) SeaKem Gold Agarose (Westburg) to form plugs. These were incubated in 2 mL of EC lysis buffer and 10 µL of proteinase K (20 mg/mL) for 2h at 55°C. The plugs were washed five times at 55°C for 15 min with sterile water, and digested overnight at 37°C with 50 U of *XbaI* (Life Technologies). Plug slices were placed on the well comb, and tempered agarose was poured in the gel mould. The gel

was run at 6.0 V/cm with an initial switch time of 5 s to a final switch time of 35 s at 14°C in 0.5× TBE (Tris-borate-EDTA) running buffer for 24 h. DNA band profiles were stained with ethidium bromide, and visualized and digitized by the Quantity One documentation system (Bio-Rad). Conversion, normalization and analysis of patterns was carried out using GelCompar software version 4.0 (Applied Maths, Kortrijk, Belgium) and pattern analyses were performed as described. [16]

WGM

The complete genomes of all 12 strains were mapped employing the Argus® Whole Genome Mapping System (Opgen Inc, Gaithersburg, USA). DNA extraction, DNA quality control, DNA restriction using *AflII*, and loading on a MapCard were done according to manufacturer's protocols. Briefly, *K. pneumoniae* colonies grown overnight at 37°C on Mueller-Hinton agar plates were immobilized in agarose plugs (as described for the PFGE protocol) and subjected to in-plug gentle lysis, followed by thoroughly washing plugs in TE buffer at 42°C and enzymatic treatment with β-agarose (New England Biolabs Inc, Ipswich, USA). For WGM, dilutions were prepared with dilution buffer, and DNA was checked for quality and presence of high molecular weight DNA molecules (Argus® QCard kit, Opgen) and subsequently loaded on the MapCard (Argus® MapCard II kit, Opgen, Inc). *De novo* assembly of restricted DNA fragments was performed using MapManager software (Opgen). For editing, maps were adjusted in orientation and in their replication point employing an *in silico* map generated from *K. pneumoniae* KPNIH31 (accession number CP009876.1) using built-in function with default parameters in MapSolver (Opgen Inc.). All WGMs were analysed by filtering out fragment sizes smaller than 5 kb from the analysis and using three different set of parameters that allowed clustering, sub-clustering, and discrepant analysis. Firstly, pattern search was performed with a relative tolerance of 5%, an absolute tolerance of 2000 (bp) with 1 mismatch and secondary criteria with most identical matches, and a similarity co-efficient set at 95% was utilised. Secondly, relative tolerance of 1%,

absolute tolerance of 1000 bp, pattern length search with 8 fragments to generate a dendrogram with most identical matches, and a similarity co-efficient of 99% was utilised. Thirdly, the same parameters as the second analysis were utilised, but instead of similarity, we studied the 'absolute number of unmatched fragments' between two WGMs assigning ≥ 10 unmatched fragments as a cut-off to assign a new cluster. All pattern-search cluster-analysis was performed using Bionumerics v7.5 (Applied Maths, Kortrijk, Belgium) employing UPGMA, and similarity matrix of clusters was defined by Cophenetic Correlation Coefficient (CCC).[17]

In silico restriction mapping using AflII

For two strains, TGH8 and TGH10, which were whole genome sequenced (see below), we performed *in silico* restriction mapping in order to quantify the fragment losses and other differences observed with experimentally-generated mapping using WGM. Comparison of *in silico* and experimentally-generated maps of the clinical strains was performed using MapSolver and BioNumerics v7.5.

WGS and comparative genome analysis

Two *K. pneumoniae* isolates (TGH8 and TGH10) were whole genome sequenced. Briefly, genomic DNA was extracted using MasterPure™ DNA Purification Kit (Epicentre Technologies Corp). WGS was performed using Nextera XT DNA Library Preparation Kit followed by sequencing via 2 X 150 bp paired end sequencing (Illumina Inc.). The sequence reads of strains were *de novo* assembled using SPAdes, [18] and annotated using Rapid Annotation Subsystem technology (RAST) online server. [19, 20] *De novo* assembled contigs were aligned against corresponding whole genome maps in MapSolver in order to generate pseudo chromosomes and also to identify variable regions and genomic content. To precisely localize the site and characteristics of the genomic change, sequence contigs corresponding to the regions of genome divergence were further analysed in CLC Genomics Workbench v7.5.1 (CLCbio, Denmark). Similarity search of variable regions was performed using NCBI BLAST at nucleotide and protein

level. [21-23] Integron (In) sorting and analysis was done as follows: *de novo* assembled contigs were sorted by length and coverage i.e., >1 kb and > 250-fold coverage, the raw reads were extracted separately, and *de novo* assembled using SPAdes. The reads were mapped again in order to validate mis-assemblies using CLC Genomics Workbench (CLCbio), and the contigs annotated and validated using online databases RAC: (Repository of Antibiotic Resistance Cassettes http://rac.aihi.mq.edu.au/rac/) and INTEGRALL.[24,25] Identification and typing of integrative and conjugative elements (ICEs) was performed using web-based resource ICEberg.[26] Plasmid sequence analysis was done as follows. Firstly, the contigs were screened for plasmid origin by using the online tool "Plasmid finder" (https://cge.cbs.dtu.dk/services/PlasmidFinder/).[27] Next, the generated plasmid-specific contigs were used as a reference template and raw reads were mapped. Lastly, *de novo* assembly was performed on the mapped reads using CLC Genomics Workbench v7.5.1 (CLCbio, Denmark) with default parameters.

RESULTS

Phenotypic and genotypic characterization of K. pneumoniae

Twelve of the 11 strains were carbapenem-resistant of which 7 harboured *bla*$_{\text{KPC-2}}$ and 11 *bla*$_{\text{VIM-19}}$ (Table 1). The ST383 strains exhibited five carbapenemase/ESBL combinations: 1) *bla*$_{\text{VIM-19}}$, *bla*$_{\text{KPC-2,}}$ and *bla*$_{\text{CTX-M-15}}$ (TGH1, TGH6, TGH8, TGH9), 2) *bla*$_{\text{VIM-19}}$, and *bla*$_{\text{KPC-2}}$ (TGH2, TGH4, andTGH5), 3) *bla*$_{\text{VIM-19}}$, and *bla*$_{\text{CTX-M-15}}$ (TGH3), 4) *bla*$_{\text{CTX-M-15}}$ (TGH7) and 5) *bla*$_{\text{VIM-19}}$ (TGH10, TGH11 and TGH12) (Table 1).

Genetic diversification within K. pneumoniae ST383 identified by WGM

Strains TGH1-TGH12 belonged to ST383 and were divided into 3 PFGE types based on a ≥ 7-band difference. Subtypes were delineated based on a ≥ 3-band difference between profiles belonging to the same PFGE type (Figure 1). Utilizing a similarity co-efficient cut-off of 95% and TGH1, the oldest strain in our collection, as the reference map, WGMs of all 12 ST383 strains were found to form 1 cluster (Figure 2). TGH8 and TGH9 showed maximum dissimilarity (4.7%) compared to the other 10 strains (Figure 2). Differences between strains were mainly due to presence of mobile elements such as ICEs, prophages, and transposons. To add further granularity to our data and observe sub-clusters, we analysed the WGMs using more stringent parameters (Figure 3A and B). Figure 3A shows clustering based on a similarity co-efficient of 99% and Figure 3B using a diversity co-efficient (no. of unmatched fragments). Both parameters showed similar (sub) clustering of WGMs, identifying two clusters, C1 and C2, and two singletons, C3 and C4 (Figure 3B), with C1 and C2 each divided into two sub clusters and a singleton (Figure 3B). In this analysis, TGH9 was found to be the most dissimilar strain showing only 77.4% similarity or a 124-unmatched fragment difference with the rest of the WGMs (Figure 3A and B). Insertions in TGH8 and TGH11, identified by WGM analysis, accounted for ~1.8% and ~1.2 % genomic expansion (Figure 3A), respectively, compared to the other ST383 strains studied here.

193 *Comparison of discriminatory power and congruence between WGM and PFGE*

194 We utilized the adjusted Wallace co-efficient to compare partitions, and the Simpson's diversity
195 index (SDI) to compare the discriminatory power of WGM and PFGE.[28] As all strains studied here
196 belonged to one ST type (ST383), no. of partitions achieved with MLST was 1 and hence was not
197 included in this analyses. Based on the parameter 'no. of unmatched fragments' ≥10 (or distance
198 co-efficient) (Figure 3B), we obtained 8 (sub) clusters with WGM that were compared to the
199 corresponding 3 PFGE types (≥ 7-band difference) and 8 subtypes (≥ 3-band difference). Based on
200 a ≥3-band difference between PFGE profiles, no significant difference was observed in the SDI of
201 WGM (0.94, Jackknife pseudo-values CI: 0.883-0.996) and PFGE (0.93, Jackknife pseudo-values
202 CI: 0.828-1.000) (p = 0.649). The adjusted Wallace co-efficient was also similar for PFGE (0.36,
203 95% CI: 0.000-0.816, ≥ 3-band difference) and WGM (0.46, 95% CI: 0.076-0.842). However,
204 discriminatory power of WGM was significantly higher (SDI: 0.94, Jackknife pseudo-values CI:
205 0.883-0.996) than PFGE based on a ≥7-band difference (SDI: 0.53, Jacknife pseudo-values CI:
206 0.212-0.849) (p = 0.007).

207 *Comparing experimentally derived WGM with in-silico restriction mapping using AflII*

208 In order to assess the reliability and accuracy of the experimentally derived WGMs, we compared
209 these with *in silico AflII* restriction maps generated from the whole genome sequencing data of
210 TGH8 and TGH10 (Figure 4A). *AflII*, the manufacturer recommended and optimized enzyme for
211 *K. pneumoniae* produces 442 (TGH8) and 437 (TGH10) fragments ranging from 78 kb-14 nt.
212 After removal of the <5 kb fragment differences, we observed a similarity co-efficient of 80-84%
213 between the experimental and *in silico* maps (Figure 4A). A similar comparison between PFGE
214 and *XbaI in silico* restriction mapping was not possible because of the basic difference in map
215 generation; the former being molecular size based fragmentation and the latter an ordered genome
216 map. Nonetheless, *XbaI in silico* restriction mapping of TGH8 and TGH10 produced
217 approximately 45 and 37 fragments respectively (data not shown), while their respective PFGE

profiles showed 17 and 15 fragments, respectively, with the < 36 kb fragments lost to follow-up on PFGE gels (Figure 1).

Comparison of TGH8 experimental and *in silico* maps showed that there were missing restriction cuts in the former (Figure 4B). The TGH8 *in silico* map generated a total of 442 *AflII*-restricted fragments of which 284 were >5 kb, while the experimental map showed a total of 386 fragments of which 278 were > 5 kb. Similarly, the TGH10 *in silico* map generated a total of 437 *AflII*-restricted fragments of which 282 were >5 kb, while the experimental map showed a total of 385 fragments of which 278 were > 5 kb.

Intra-cluster comparison of ST383 whole genome maps

Compared to the other ST383 maps, TGH11 and TGH8 showed two unique insertions of ~31 kb and ~110 kb, respectively (Figure 2). These genomic insertions were unique in our mapped strains as deduced from comparative analysis of TGH8 and TGH11 maps with *in silico* maps generated from six previously sequenced *K. pneumoniae* available on NCBI (data not shown). By aligning the pseudo chromosomes of TGH8 and TGH10 to their corresponding WGMs, it was possible to pinpoint the sequence region harbouring the insertion in TGH8. The TGH8 insertion (from 773,512, to 884,869 kb) was identified as 99% homologous to a region present in *Proteus mirabilis* strain HI4320 (2,793,662 to 2,886,224 kb, accession number: AM942759). In TGH8, the ~110 kb genomic insertion lies in a region of high plasticity as evidenced by presence of flanking phage and mobile element remnants such as genes encoding phage capsids, phage-associated hypothetical proteins as well as transposases. Our search of the ~110 kb insertion against the ICEberg database identified an unclassified ~94 kb *ICEPm1* element, which harbours genes encoding a putative signal transducer/ampG/MFS, and virulence-associated genes such as F17 fimbrial protein precursor, iron acquisition yersiniabactin synthesis enzyme, soluble lytic murine transglycosylase, type IV secretory pathway VirD4/B4, and interestingly, a lipid A export ATP-binding protein/MsbA. Similar searches for the ~ 31 kb insertion in TGH11 did not identify any

pathogenic or virulence-related determinants in this region but rather genes encoding for glucan biosynthesis protein D precursor, permeases of drug/metabolite transporter (DMT), tellurite resistance proteins (TehA/TehB), benzyl alcohol dehydrogenase, and an uncharacterized membrane lipoprotein (data not shown).

Analysis of integrons harbouring bla_{VIM} variants

Integron analysis of our sequenced strains (TGH8 and TGH10) showed that $bla_{\text{VIM-19}}$ in both TGH8 and TGH10 was carried on the class 1 integron, *In4863*, which showed 99% nucleotide level similarity between TGH8 and TGH10 (Figure 5). However, in contrast to the previously sequenced *In4863* (accession number KF894700), the element in TGH8 and TGH10 harboured a variant promoter (PcW-TGN-10),[29] showing polymorphism at the 2nd base of the -35 sequence (T**T/G**ACA). In addition, Int1 also showed two predicted amino acid changes (Pro32Arg and Asn39His) compared to the published *In4863* sequence (Figure 5).

In silico analysis of plasmid specific contigs using Plasmid finder and comparative sequence analysis showed that $bla_{\text{KPC-2}}$, $bla_{\text{CTX-M}}$ and $bla_{\text{VIM-19}}$ were might be carried on three different plasmids (IncFII(K), IncFIB and IncA/C2, respectively) in TGH8.

DISCUSSION

In this study, we utilized a collection of carbapenem-resistant *K. pneumoniae* isolated during 2010-2013 at the TG hospital, Greece in order to compare currently utilised gene- and genome-based typing methods as well as to better understand the molecular epidemiology of carbapenem-resistant *K. pneumoniae* at TGH.

MLST assigned all strains studied here to ST383. In concordance, a cut-off of 95% similarity co-efficient also assigned all WGMs to a single cluster. To allow comparisons with PFGE, which assigned the ST383 to 3 types based on a ≥ 7-band difference and to 8 subtypes based on a ≥ 3 band difference, we utilized a '≥ 10 unmatched fragment' criteria to assign WGM clusters. Compared to a ≥ 7-band difference in PFGE profiles, WGM showed a significantly higher discriminatory power while a 3- band difference criteria showed a similar SDI for PFGE and WGM. Different restriction enzymes had to be employed for these methods; *AflII* is the manufacturer recommended enzyme for whole genome mapping of *K. pneumoniae*, however fragment sizes with this enzyme range from 78 kb to14 nt. As a large number of *AflII*-generated fragments fall below the resolution of PFGE gels (<36 kb fragments in our hands, Figure 1), we utilized *XbaI* for the latter method. *In silico* mapping of TGH8 with *AflII* and *XbaI* generated 442 and 45 (556 kb to 197 nt) fragments, respectively. However, on-gel *XbaI* PFGE profiles consisted of, on average, 14 bands. Comparison of experimental and *in silico* maps also highlighted the challenges WGM faces for scoring of small fragments. Of the 56 and 52 missing fragments in the TGH8 and TGH10 experimental WGMs compared to their *in silico* maps, 50 and 48 (11% for both) were < 5 kb, respectively. This corresponds to a small fragment loss of 32%. In contrast, fragment loss rate of > 5 kb fragments was only 1.4-2.1% for both TGH8 and TGH10 WGMs. Despite lack of evident differences in discriminatory power between PFGE and WGM, which might be due to the fact that the number of strains analysed here were limited and were closely related, a major advantage of WGM is that the technique produces an ordered genome map that

allows comparison to previously sequenced genomes for identifying larger (> 5 kb) insertions/deletions. For instance, prior to sequencing, we had already identified the insertion observed in the WGM of TGH8 as an *ICEPm1* element by comparing with *in silico* maps generated from six previously sequenced *K. pneumoniae* available on NCBI. This element has been shown to originate from *P. mirabilis*, and is also highly conserved in other uropathogens such as *Providencia stuartii* and *Morganella morganii.*[30] Interestingly, the *ICEPm1* element is known to transfer in a site-specific manner, using phenylalanine tRNA genes as an integration site, [31] and may contribute to fine tuning and adaptation of *K. pneumoniae* towards preferred infection or colonization pathways.[32]

ST383 is a recently described clone that was first detected in Greek hospitals during 2009-2010.[33] Majority of the ST383 strains circulating in various Greek hospitals during 2009-2010 reportedly co-harboured $bla_{\text{VIM-4}}$, $bla_{\text{KPC-2}}$ and $bla_{\text{CMY-4}}$ β-lactamases.[33] Recent studies of 1-3 isolates of ST383 *K. pneumoniae* recovered during 2008-2010 have also reported presence of $bla_{\text{VIM-19}}$ in this ST type.[34, 35] ST383 strains isolated at TGH in 2010-11 harboured the $bla_{\text{VIM-19}}$, bla_{KPC-2} and $bla_{CTX-M-15}$ plasmids in various combinations, while one isolate that was carbepenem-susceptible did not harbour a carbapenemase. On the other hand, strains isolated in 2013 (TGH10,TGH11 and TGH12) harboured only $bla_{\text{VIM-19.}}$ These data underscore the remarkable plasticity of ST383 in terms of the accessory genome. Subject to the limited high-level MIC resolution allowed by Etest, carbapenem resistance remained high in the TGH10, TGH11 and TGH12 isolates despite loss of bla_{KPC-2}, and potentiates the possibility that plasmid loss might have benefitted the ST383 strains in terms of fitness and transmissibility.

The $bla_{\text{VIM-19}}$ carbapenemase is also a new metallo-β-lactamase (MBL) gene variant isolated in Algiers in 2009.[36] It is known to be derived from $bla_{\text{VIM-1}}$, differing from the former by two substitutions: Ser228Arg and Asn215Lys,[36] which confer higher resistance to the carbapenems in comparison to $bla_{\text{VIM-1}}$.[37] Accordingly, all $bla_{\text{VIM-19}}$ harbouring ST383 in this study, irrespective of

the presence of *bla*$_{KPC-2}$, showed high-level resistance to meropenem, imipenem and ertapenem. Pournaras *et al.* have reported presence of *bla*$_{VIM-19}$ in a *K. pneumoniae* clinical strain co-producing *bla*$_{KPC-2}$ carbapenemase, *bla*$_{CMY-2}$ cephalosporinase and *bla*$_{CTX-M-15}$ extended-spectrum β-lactamase.[38] They found the *bla*$_{VIM-19}$ gene to be associated with a new class 1 integron with a structure similar to that carrying the close variant gene *bla*$_{VIM-4}$ in an *Enterobacter cloacae* isolate from Greece.[38] The *bla*$_{VIM-19}$ gene cassette was located downstream of the *attI1* recombination site, followed by an *aacA6* cassette, a *dfrA1* cassette, an *aadA1* cassette and the 3′-CS, containing *qacEΔ1* and *sulI*.[38] Another study has shown *bla*$_{VIM-19}$ to be harboured on *In4863*.[35] In our *In4863*-like element, the *bla*$_{VIM-19}$ gene cassette was located downstream of the *attI1* recombination site, followed by an *aacA6* cassette, a *dfrA1b/15* cassette, an *aad*Δ*A1* cassette and the Δ*smr2/sugE* (Quaternary ammonium compound-resistance protein) truncated by *ISPa21*. Furthermore, the *In4863*-like element differed from the previously described *In4863* by two (predicted) amino acid substitutions in the integrase and one nucleotide change at the 2nd position (T>G) in the integron promoter sequence. Interestingly, a recent study showed that these changes result in increased integrase activity and a concomitant decrease in promoter strength,[29] which hypothetically would increase the frequency of recombination events and acquisition of novel gene cassettes by the *In4863*-like element under antibiotic pressure. Also, the proximity of the gene cassette to the integron promoter influences its expression; closer the gene cassette to the promoter higher the expression. An *in vitro* study analysed the impact of chloramphenicol pressure on gene cassette rearrangements in a class 1 integron harbouring the chloramphenicol-resistance encoding *catB9* gene, and found a wide variety of rearrangements under chloramphenicol pressure all leading to increased proximity of *catB9* to the integron promoter.[39] Remarkably, all known MBL gene cassettes, including those harbouring *bla*$_{VIM-19}$, have been found to be consistently placed next to the integron's promoter.[35, 40] Sustained carbapenem use and selection pressure in hospital

environments are likely responsible for maintenance of MBL gene cassettes in this priority position.

To conclude, this study demonstrated the application of whole genome mapping to understanding the epidemiology of hospital-associated *K. pneumoniae*. Additionally, a combination of whole genome mapping and sequencing provided novel insights on the genomic features of the multi-drug resistant ST383 *K. pneumoniae* clone that is rapidly gaining importance in terms of prevalence and clinical significance in Europe.

Acknowledgements

The authors thank Sabine Chapelle for providing excellent technical assistance.

Funding

This work was partly financially supported by EU grants, RGNOSIS (Resistance in Gram-Negative Organisms: Studying Intervention Strategies, FP7 HEALTH.2011.2.3.1-3, #282512), and PREPARE (Platform foR European Preparedness Against (Re-)emerging Epidemics, EU-FP7, # 602525), and by Opgen Inc., Gaithersburg, USA in the framework of the European Public Health Initiative (EUPHi). B.B.X. is supported by University of Antwerp Research Funds (BOF-DOCPRO 2012-27450).

Transparency declarations

The authors declare no transparency declarations

Genbank depositions

The accession numbers for the integron (*In4863*-like) and whole genome sequences deposited in Genbank are as follows; *In4863*-like (KT820212), TGH8 (CP012743) and TGH10 (CP012744).

References

1. Mathers AJ, Cox HL, Kitchel B et al. Molecular Dissection of an Outbreak of Carbapenem-Resistant Enterobacteriaceae Reveals Intergenus KPC Carbapenemase Transmission through a Promiscuous Plasmid. *mBio* 2011; **2**: e00204-11.
2. Stapleton PD, Shannon KP, French GL. Carbapenem resistance in Escherichia coli associated with plasmid-determined CMY-4 beta-lactamase production and loss of an outer membrane protein. *Antimicrobial agents and chemotherapy* 1999; **43**: 1206-10.
3. Goren MG, Carmeli Y, Schwaber MJ et al. Transfer of carbapenem-resistant plasmid from Klebsiella pneumoniae ST258 to Escherichia coli in patient. *Emerging infectious diseases* 2010; **16**: 1014-7.
4. Saidel-Odes L, Borer A. Limiting and controlling carbapenem-resistant Klebsiella pneumoniae. *Infection and drug resistance* 2013; **7**: 9-14.
5. Miller JM. Whole-genome mapping: a new paradigm in strain-typing technology. *J Clin Microbiol* 2013; **51**: 1066-70.
6. Miyakis S, Pefanis A, Tsakris A. The Challenges of Antimicrobial Drug Resistance in Greece. *Clinical Infectious Diseases* 2011; **53**: 177-84.
7. Poulou A, Spanakis N, Pournaras S et al. Recurrent healthcare-associated community-onset infections due to Klebsiella pneumoniae producing VIM-1 metallo-β-lactamase. *Journal of Antimicrobial Chemotherapy* 2010; **65**: 2538-42.
8. Pournaras S, Protonotariou E, Voulgari E et al. Clonal spread of KPC-2 carbapenemase-producing Klebsiella pneumoniae strains in Greece. *Journal of Antimicrobial Chemotherapy* 2009; **64**: 348-52.
9. Maltezou HC, Giakkoupi P, Maragos A et al. Outbreak of infections due to KPC-2-producing Klebsiella pneumoniae in a hospital in Crete (Greece). *Journal of Infection* 2009; **58**: 213-9.
10. Giakkoupi P, Pappa O, Polemis M et al. Emerging Klebsiella pneumoniae Isolates Coproducing KPC-2 and VIM-1 Carbapenemases. *Antimicrobial agents and chemotherapy* 2009; **53**: 4048-50.
11.Clinical and Laboratory Standards Institute. *Performance Standards for Antimicrobial Susceptibility Testing: 24nd Informational Supplement M100-S24.* CLSI, Wayne, PA, USA, 2014.
12. Monstein HJ, ÖStholm-Balkhed Å, Nilsson MV et al. Multiplex PCR amplification assay for the detection of blaSHV, blaTEM and blaCTX-M genes in Enterobacteriaceae. *APMIS* 2007; **115**: 1400-8.
13. Poirel L, Walsh TR, Cuvillier V et al. Multiplex PCR for detection of acquired carbapenemase genes. *Diagnostic microbiology and infectious disease* 2011; **70**: 119-23.
14. Mabilat C, Goussard S, Sougakoff W et al. Direct sequencing of the amplified structural gene and promoter for the extended-broad-spectrum beta-lactamase TEM-9 (RHH-1) of Klebsiella pneumoniae. *Plasmid* 1990; **23**: 27-34.
15. Diancourt L, Passet V, Verhoef J et al. Multilocus sequence typing of Klebsiella pneumoniae nosocomial isolates. *J Clin Microbiol* 2005; **43**: 4178-82.
16. Tenover FC, Arbeit RD, Goering RV et al. Interpreting chromosomal DNA restriction patterns produced by pulsed-field gel electrophoresis: criteria for bacterial strain typing. *J Clin Microbiol* 1995; **33**: 2233-9.
17. Boopathi NM, & SpringerLink (Online service). . *Genetic mapping and marker assisted selection: Basics, practice and benefits*: Springer India, 2013.
18. Bankevich A, Nurk S, Antipov D et al. SPAdes: a new genome assembly algorithm and its applications to single-cell sequencing. *Journal of computational biology : a journal of computational molecular cell biology* 2012; **19**: 455-77.
19. Aziz RK, Bartels D, Best AA et al. The RAST Server: Rapid Annotations using Subsystems Technology. *BMC Genomics* 2008; **9**: 75-.

20. Overbeek R, Olson R, Pusch GD et al. The SEED and the Rapid Annotation of microbial genomes using Subsystems Technology (RAST). *Nucleic Acids Research* 2014; **42**: D206-D14.
21. Altschul SF, Gish W, Miller W et al. Basic local alignment search tool. *Journal of molecular biology* 1990; **215**: 403-10.
22. States DJ, Gish W. Combined use of sequence similarity and codon bias for coding region identification. *Journal of computational biology : a journal of computational molecular cell biology* 1994; **1**: 39-50.
23. Cosentino S, Voldby Larsen M, Møller Aarestrup F et al. PathogenFinder - Distinguishing Friend from Foe Using Bacterial Whole Genome Sequence Data. *PloS one* 2013; **8**: e77302.
24. Tsafnat G, Copty J, Partridge SR. RAC: Repository of Antibiotic resistance Cassettes. *Database* 2011; **2011**.
25. Moura A, Soares M, Pereira C et al. INTEGRALL: a database and search engine for integrons, integrases and gene cassettes. *Bioinformatics* 2009; **25**: 1096-8.
26. Bi DX, Xu Z, Harrison EM et al. ICEberg: a web-based resource for integrative and conjugative elements found in Bacteria. *Nucleic Acids Research* 2012; **40**: D621-D6.
27. Carattoli A, Zankari E, García-Fernández A et al. In Silico Detection and Typing of Plasmids using PlasmidFinder and Plasmid Multilocus Sequence Typing. *Antimicrobial agents and chemotherapy* 2014; **58**: 3895-903.
28. Carriço JA, Silva-Costa C, Melo-Cristino J et al. Illustration of a Common Framework for Relating Multiple Typing Methods by Application to Macrolide-Resistant Streptococcus pyogenes. *Journal of Clinical Microbiology* 2006; **44**: 2524-32.
29. Jové T, Da Re S, Denis F et al. Inverse Correlation between Promoter Strength and Excision Activity in Class 1 Integrons. *PLoS Genet* 2010; **6**: e1000793.
30. Flannery EL, Mody L, Mobley HLT. Identification of a Modular Pathogenicity Island That Is Widespread among Urease-Producing Uropathogens and Shares Features with a Diverse Group of Mobile Elements. *Infection and Immunity* 2009; **77**: 4887-94.
31. Flannery EL, Antczak SM, Mobley HLT. Self-Transmissibility of the Integrative and Conjugative Element ICEPm1 between Clinical Isolates Requires a Functional Integrase, Relaxase, and Type IV Secretion System. *J Bacteriol* 2011; **193**: 4104-12.
32. Chen N, Ou H-Y, van Aartsen J et al. The pheV Phenylalanine tRNA Gene in Klebsiella pneumoniae Clinical Isolates Is an Integration Hotspot for Possible Niche-Adaptation Genomic Islands. *Curr Microbiol* 2010; **60**: 210-6.
33. Papagiannitsis CC, Giakkoupi P, Vatopoulos AC et al. Emergence of Klebsiella pneumoniae of a novel sequence type (ST383) producing VIM-4, KPC-2 and CMY-4 beta-lactamases. *International journal of antimicrobial agents* 2010; **36**: 573-4.
34. Samuelsen Ø, Toleman MA, Hasseltvedt V et al. Molecular characterization of VIM-producing Klebsiella pneumoniae from Scandinavia reveals genetic relatedness with international clonal complexes encoding transferable multidrug resistance. *Clinical Microbiology and Infection* 2011; **17**: 1811-6.
35. Papagiannitsis CC, Izdebski R, Baraniak A et al. Survey of metallo-β-lactamase-producing Enterobacteriaceae colonizing patients in European ICUs and rehabilitation units, 2008–11. *Journal of Antimicrobial Chemotherapy* 2015; **70**: 1981-8.
36. Robin F, Aggoune-Khinache N, Delmas J et al. Novel VIM Metallo-β-Lactamase Variant from Clinical Isolates of Enterobacteriaceae from Algeria. *Antimicrobial agents and chemotherapy* 2010; **54**: 466-70.
37. Rodriguez-Martinez J-M, Nordmann P, Fortineau N et al. VIM-19, a Metallo-β-Lactamase with Increased Carbapenemase Activity from Escherichia coli and Klebsiella pneumoniae. *Antimicrobial agents and chemotherapy* 2010; **54**: 471-6.

38. Pournaras S, Poulou A, Voulgari E et al. Detection of the new metallo-β-lactamase VIM-19 along with KPC-2, CMY-2 and CTX-M-15 in Klebsiella pneumoniae. *Journal of Antimicrobial Chemotherapy* 2010; **65**: 1604-7.
39. Barraud O, Ploy M-C. Diversity of Class 1 Integron Gene Cassette Rearrangements Selected Under Antibiotic Pressure. *J Bacteriol* 2015.
40. Zhao W-H, Hu Z-Q. Acquired metallo-β-lactamases and their genetic association with class 1 integrons and ISCR elements in Gram-negative bacteria. *Future Microbiology* 2015; **10**: 873-87.

Legends to Figures and Tables

Figure 1. PFGE types (≥ 7-band difference) and subtypes (≥ 3-band difference) of *K. pneumoniae* ST383

Figure 2. Comparison of whole genome maps of ST383 strains. Green shaded areas indicate identical restriction patterns among the maps and red horizontal marks represent variations. A similarity co-efficient of 95% was utilised which assigned the strain to a single cluster.

Figure 3. Comparison of whole genome maps of ST383 strains using a similarity coefficient of 99% **(A)**, and a '≥ 10 unmatched fragments' criterion **(B).** Both parameters showed similar (sub) clustering of WGMs, identifying two clusters (C1 and C2) and two singletons (C3 and C4) with C1 and C2 each divided into two sub clusters and a singleton.

Figure 4. Comparison of experimental and *in silico* restriction maps using *AflII* that show fragment losses ranging from 28 kb to 43 kb in both experimental and *in silico* maps **(A)**. Comparison of zoomed-in experimental and *in silico* restriction map of TGH8 showing missing restriction enzyme cuts in the former **(B)**.

Figure 5. Gene cassette arrangement in Class 1 integrons harboured by ST383 (*In4863*-like) and Int1 protein alignment. Amino acids boxed in black represent variation in the Int1 protein between TGH8 and TGH10 ST383 compared to published Class 1 integrases.

Table 1. Clinical data and characteristics of strains under study

Strain ID	Clinical information			Molecular typing								Resistance profile											
	Unit	Site of isolation	Isolation date	PFGE*	ST type	WGM Type	*bla*-genes					MIC by E test						Sensitivity by Disk Diffusion**					
							bla_{VIM}	bla_{KPC}	bla_{CTX-M}	bla_{SHV}	bla_{TEM}	Meropenem		Ertapenem		Imipenem		Fosfomycin		Cefoxitin		Gentamicin	
TGH1	ICU	Blood	Jan-10	3a	ST383	C1a	VIM-19	KPC-2	CTX-M-15	SHV-1	TEM-1	R	>32	R	>32	R	>32	S	19	R	0	R	0
TGH2	S	Wound Swab	Feb-10	1a	ST383	C2b	VIM-19	KPC-2	-	SHV-1	TEM-1	R	>32	R	>32	R	>32	S	19	R	0	S	21
TGH3	ICU	Urinary Catheter	Apr-10	1b	ST383	C1a	VIM-19	-	CTX-M-15	SHV-1	-	R	>32	R	>32	R	>32	S	19	R	0	R	0
TGH4	S	Urine	May-10	1a	ST383	C2b	VIM-19	KPC-2	-	SHV-1	TEM-1	R	>32	R	>32	R	>32	S	20	R	0	S	21
TGH5	ICU	Blood	May-10	3a	ST383	C1b	VIM-19	KPC-2	-	SHV-1	TEM-1	R	>32	R	>32	R	>32	S	19	R	0	S	22
TGH6	ICU	CVC	Aug-10	1d	ST383	C1b	VIM-19	KPC-2	CTX-M-15	SHV-1	-	R	>32	R	>32	R	>32	S	21	R	0	R	0
TGH7	S	Urine	Nov-10	1c	ST383	C2c	-	-	CTX-M-15	SHV-1	-	S	0.023	S	0,023	S	0.19	S	21	I	15	R	0
TGH8	ICU	CVC	Jun-11	2a	ST383	S3	VIM-19	KPC-2	CTX-M-15	SHV-1	TEM-1	R	>32	R	>32	R	>32	R	0	R	0	R	0
TGH9	ICU	Blood	Aug-11	3b	ST383	S4	VIM-19	KPC-2	CTX-M-15	SHV-1	TEM-1	R	>32	R	>32	R	>32	S	18	R	0	R	0
TGH10	ICU	Wound Swab	Mar-13	1b	ST383	C2a	VIM-19	-	-	SHV-1	-	R	>32	R	>32	R	>32	S	18	R	0	R	0
TGH11	ICU	Rectal	Apr-13	1e	ST383	C1c	VIM-19	-	-	SHV-1	-	R	>32	R	>32	R	>32	S	19	R	0	R	0
TGH12	S	Blood	Apr-13	1b	ST383	C2a	VIM-19	-	-	SHV-1	-	R	>32	R	>32	R	>32	S	19	R	0	R	0

*To define a PFGE type, ≥7-band difference cut-off was utilized. The number of band differences between the subtypes is 1, which indicates that the strains were genetically closely-related.

** All strains were resistant to the following antibiotics by disc diffusion: amoxicillin, piperacillin, amoxicillin-clavulanic acid, piperacillin-tazobactam, cefepime, cefotaxime, ceftazidime, aztreonam, ciprofloxacin, nitrofurantoin, trimethoprim- sulfamethoxazole.

Abbreviations: SS - surgical site, ICU - intensive care unit, CVC - central venous catheter, R – resistant, S - susceptible.

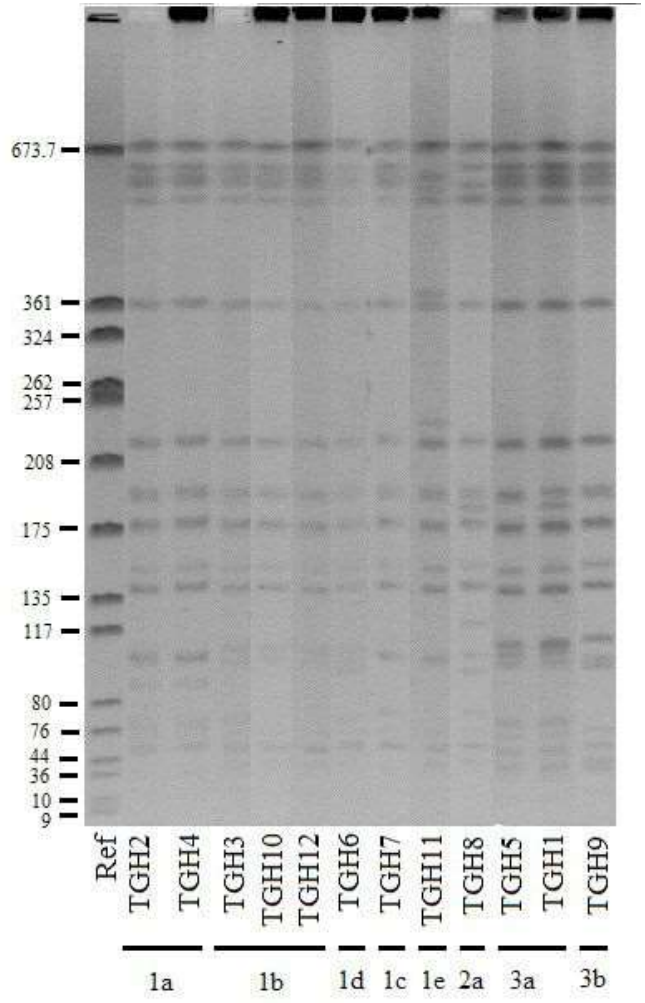
673.7
361
324
262
257
208
175
135
117
80
76
44
36
10
9
Ref
TGH2
TGH4
TGH3
TGH10
TGH12
TGH6
TGH7
TGH11
TGH8
TGH5
TGH1
TGH9
1a
1b
1d
1c
1e
2a
3a
3b

Figure 1

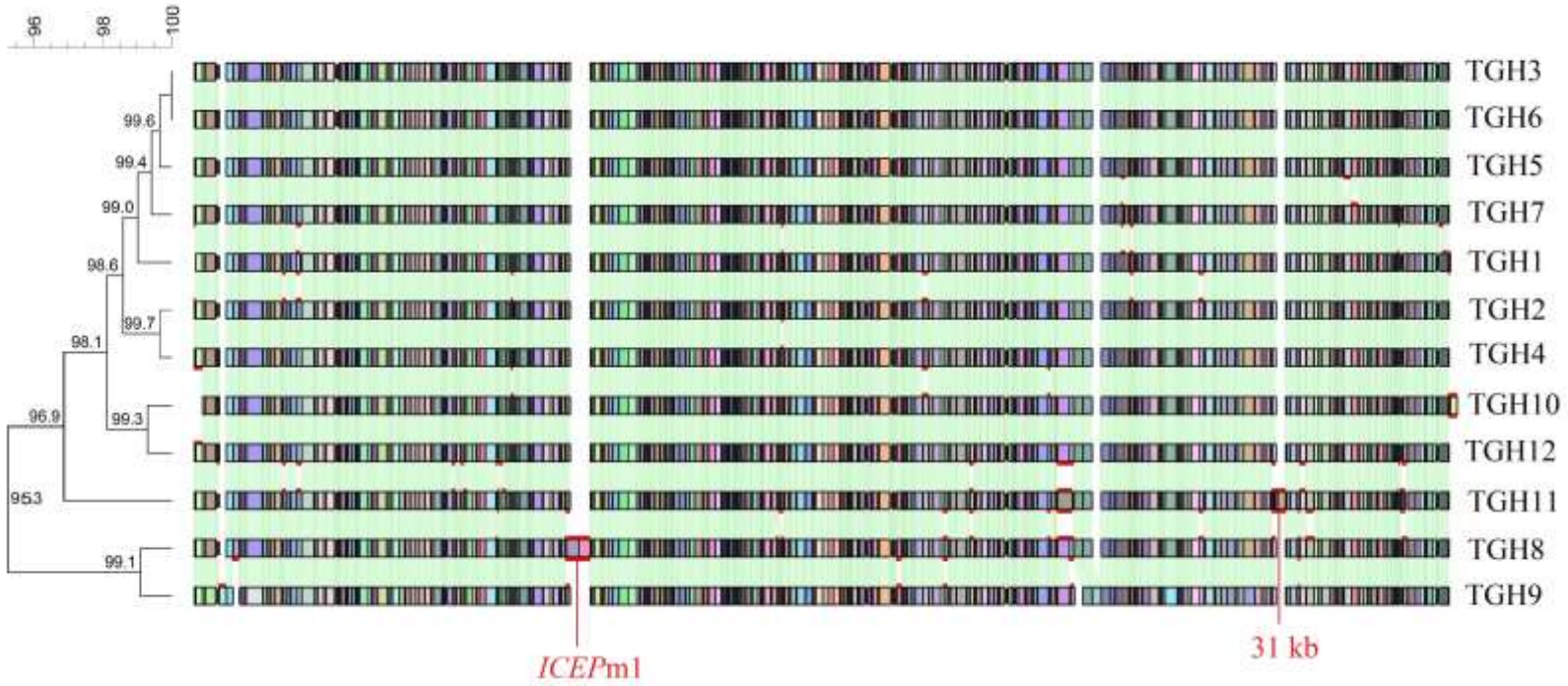
96
98
100
99.6
99.4
99.0
98.6
99.7
98.1
96.9
99.3
95.3
99.1
TGH3
TGH6
TGH5
TGH7
TGH1
TGH2
TGH4
TGH10
TGH12
TGH11
TGH8
TGH9
ICEPm1
31 kb

Figure 2


A.
80
90
100
99.3
97.4
94.1
99.3
91.8
98.2
97.2
96.3
99.3
77.4
TGH1
TGH3
TGH6
TGH5
TGH11
TGH12
TGH10
TGH7
TGH4
TGH2
TGH8
TGH9
ICEPmi
31kb
B.
100
50
0
4.0
14.5
32.5
4.0
45.4
10.0
15.7
21.0
4.0
124.0
TGH1
TGH3
TGH5
TGH6
TGH11
TGH10
TGH12
TGH7
TGH2
TGH4
TGH8
TGH9
C1a
C1b
C1c
C2c
C2a
C2b
C3
C4

Figure 3

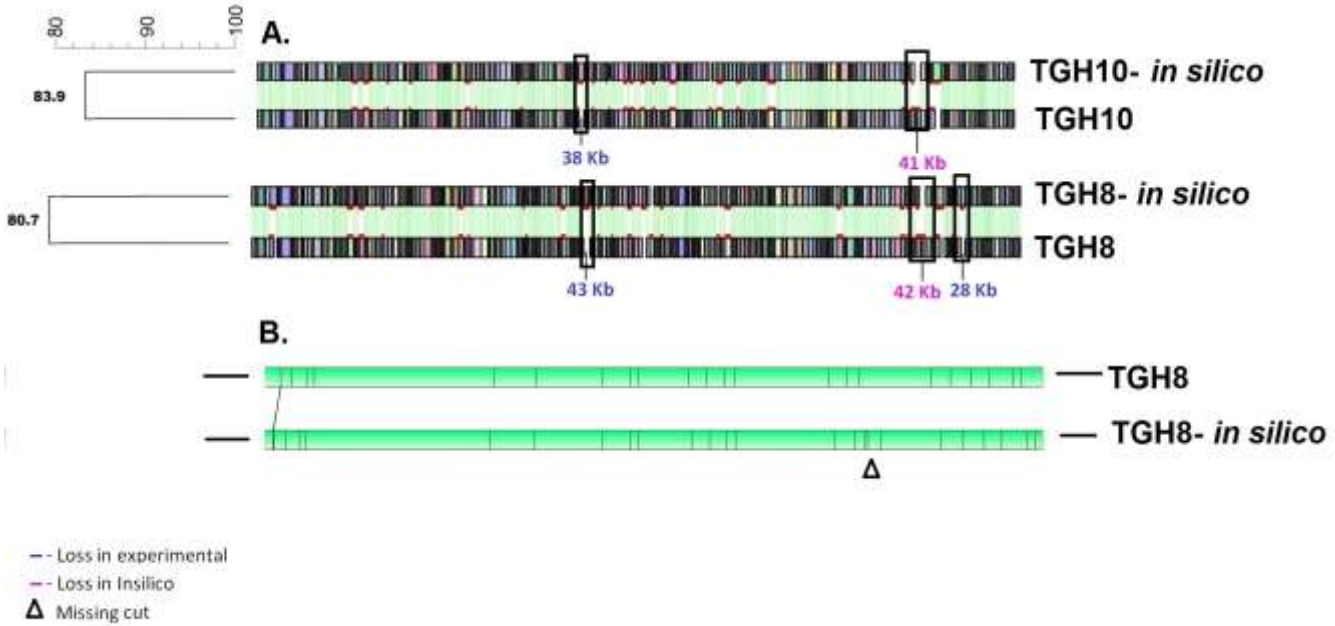
80
90
100
A.
83.9
TGH10- in silico
TGH10
38 Kb
41 Kb
80.7
TGH8- in silico
TGH8
43 Kb
42 Kb
28 Kb
B.
TGH8
TGH8- in silico
Δ
- - Loss in experimental
- - Loss in Insilico
Δ Missing cut

Figure 4

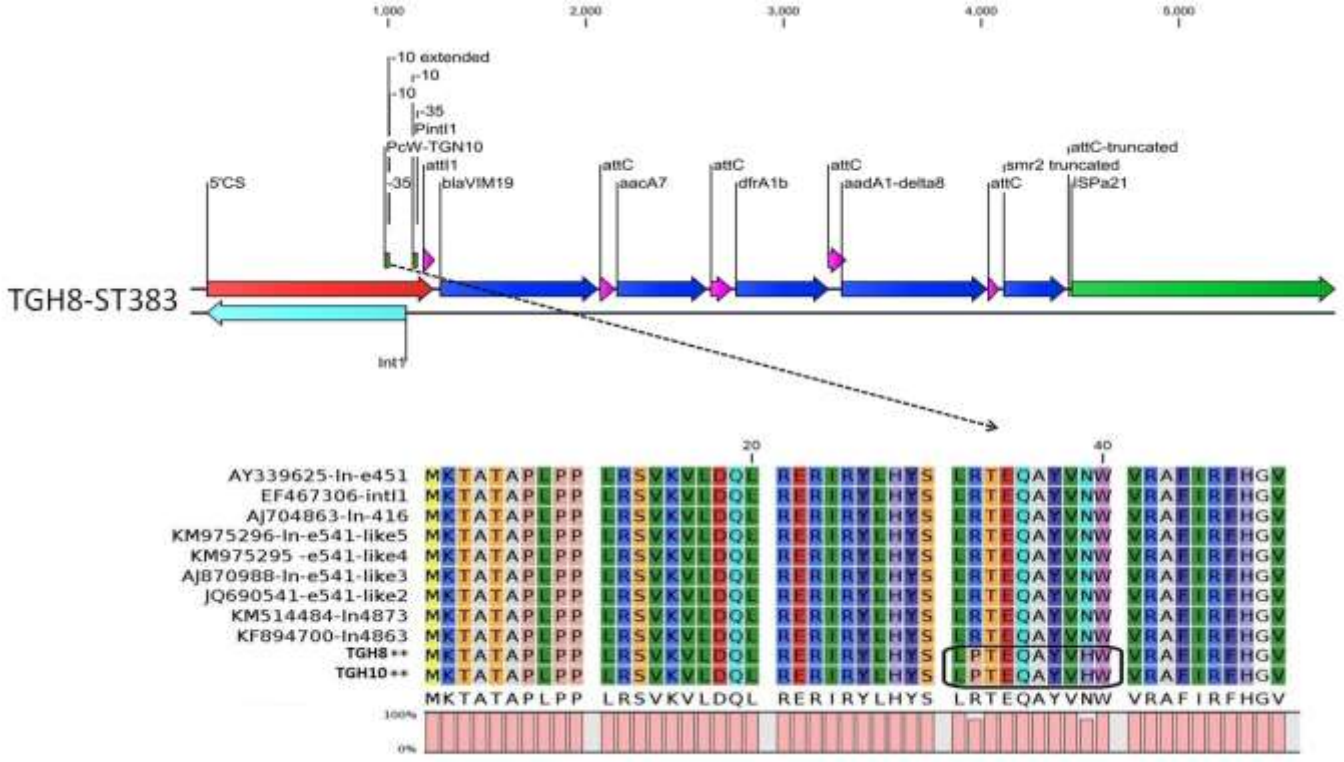
1,000
2,000
3,000
4,000
5,000
10 extended
-10
-10
-35
PintI1
PcW-TGN10
attI1
-35
5'CS
blaVIM19
attC
aacA7
attC
dfrA1b
attC
aadA1-delta8
attC
smr2 truncated
attC
ISPa21
attC-truncated
TGH8-ST383
Int1
20
40
AY339625-In-e451
EF467306-intI1
AJ704863-In-416
KM975296-In-e541-like5
KM975295 -e541-like4
AJ870988-In-e541-like3
JQ690541-e541-like2
KM514484-In4873
KF894700-In4863
TGH8 **
TGH10 **
MKTATAPLPP LRSVKVLDQL RERIRYLHYS LRTEQAYVNW VRAFIRFHGV
100%
0%

Figure 5